Available online at www.ilcpa.pl

International Letters of Chemistry, Physics and Astronomy

14 (2013) 37-43 ISSN 2299-3843

Effect on magnetic properties of zinc doped nano ferrites synthesized by precursor or method

T. Anjaneyulu[1,*], P. Narayana Murthy[2], Sk. Md. Rafi[1], Sk. Bademiya[1], G. Samuel John[3]

[1]Department of Physics, Narasaraopet Engineering College, Narasaraopet - 522 601, A.P., India
*Phone: 9160606045

[2]Department of Physics, Acharya Nagarjuna University, Guntur - 522 510, A.P., India

[3]Department of Physics, Krishnamurthy Institute of Technology & Engineering, Ghatkesar - 501 301, A.P., India

*E-mail address: anji_abi@yahoo.com

ABSTRACT

Nanocrystalline Cu-Zn ferrites have been synthesized using precursor method. Cu-Zn ferrites were formed at low temperature without any impurities. The particle sizes were observed to decrease from 60 nm to 50 nm with increasing non-magnetic Zn doping. Cu is used to decrease the sintering temperature. The X-ray diffraction (XRD) and IR analysis of Cu-Zn revealed the formation of Single-Phase Spinel structure at very low annealing temperature. The particle sizes observed from XRD is very well in agreement with SEM analysis. Cu-Zn ferrite nanoparticles were observed to be dependent on the particle size. Saturation (M_s) and Remanence (M_r) magnetization of ferrites increases due to the modifications occurred among the A-B, A-A and B-B interactions of Spinel structure. The Coercive force (H_c) decreases with increase of Zn ions concentration.

***Keywords*:** Nanoferrites; Cu-Zn ferrite; Precursor Method; Magnetic properties

1. INTRODUCTION

Ferrites are an important class of materials that have potential applications in integrated circuitry, transformer cores, magnetic recording etc (Suzuki, 2001 and Sugimoto, 1999). Ferrite nanoparticles have potential to replace bulky external magnets in current devices. The study of ferrite nanoparticles is of interest due to the fundamental differences in their magnetic properties compared to the bulk (Tanaka, 1999). Copper zinc ferrites crystallize in cubic spinel structure. The Cu-Zn ferrites nanoparticles properties can be influenced by several factors such as the chemical composition, electronic configuration, ionic radius, synthesis techniques etc (Smit and Wijn, 1959). Nanocrystalline Cu-Zn ferrite have been extensively investigated due to their potential applications in non-resonant device, radio frequency circuits, rod antennas, high quality filters, transformer cores, read/write heads for high speed digital tapes and operating devices (Pradan *et al.*, 2008; Lamani *et al.*, 2009).

Copper ferrite ($CuFe_2O_4$) is an interesting material and has been widely used for various applications, such as catalysts for environment (Tsoncheva *et al.*, 2010) gas sensor (Tao *et al.*, 2000) and hydrogen production (Faungnawakij *et al.*, 2007).

Magnetic properties of Cu ferrites vary greatly with the change chemical component and cation distribution. For instance, most of bulk $CuFe_2O_4$ has an inverse spinel structure, with 85 % Cu^{2+} occupying B sites (Zuo *et al.*, 2006), whereas $ZnFe_2O_4$ is usually assumed to be a completely normal spinel and Zn^{2+} ions preferentially occupy A sites while Fe^{3+} ions would be displaced from A sites for B sites (Yao *et al.*, 2007). Zn-substitution results to a change of cations in chemical composition and a different distribution of cations between A and B sites. Consequently the magnetic and electrical properties of spinel ferrites will change with changing cation distribution. However, there are no reports on the synthesis and characterize of Cu-Zn ferrites nanoparticles using oxalic acid precursor method in the literatures. Therefore, it would be interesting to synthesize Cu-Zn ferrite nanoparticles using precursor method and to study the structural and magnetic properties.

2. EXPERIMENTAL PROCEDURES

Nanocrystalline $Cu_{1-x}Zn_xFe_2O_4$ ($0.2 \leq x \leq 1.0$) was prepared by precursor method (Wickham, 1967 and Raghavender *et al.*, 2011). All of the chemicals were analytical grade. In a typical procedure, the copper hydrate $Cu(NO_3)_2 \cdot 6H_2O$, zinc nitrate hydrate $Zn(NO_3)_2 \cdot 6H_2O$, ferric nitrate nonhydrate $Fe(NO_3)_3 \cdot 9H_2O$ were used as starting materials.

Stoichiometric amounts of metal nitrates were dissolved in deionized water to get clear solution. The obtained aqueous solution of metal nitrates was mixed with oxalic acid in a molar ratio ranging from 1:4 to 1:0.2. The mixture solution were moved on to magnetic stirrer and stirred for 2 h at room temperature. The reaction mixtures turned by varying molar ratios 1:3 and 1:2. When the molar ratio was further lowered to 1:1, precursor solution showed different colour shades. The resultant mixtures were evaporated on a hot plate at 150 °C for 2 h. The obtained raw powders were thermally heat treated at 350 °C for 4 h to get the single phase nanocrystalline Cu-Zn ferrites. The structural characterization of the prepared Cu-Zn ferrite nanopowders was carried out using Philips X-ray diffraction system with Ni filter using Cu – Kα radiation (wave length λ = 1.54 Å). The average particle size *D* was calculated using most intense peak (311) employing the Scherer formula. The particle size and morphology was carried out using FE-SEM (model JSM-7000F) manufactured by JEOL Ltd.

Figure 1. SEM images of $Cu_{1-x}Zn_xFe_2O_4$ (a) $x = 0.2$ and (b) $x = 1.0$ nanoparticles.

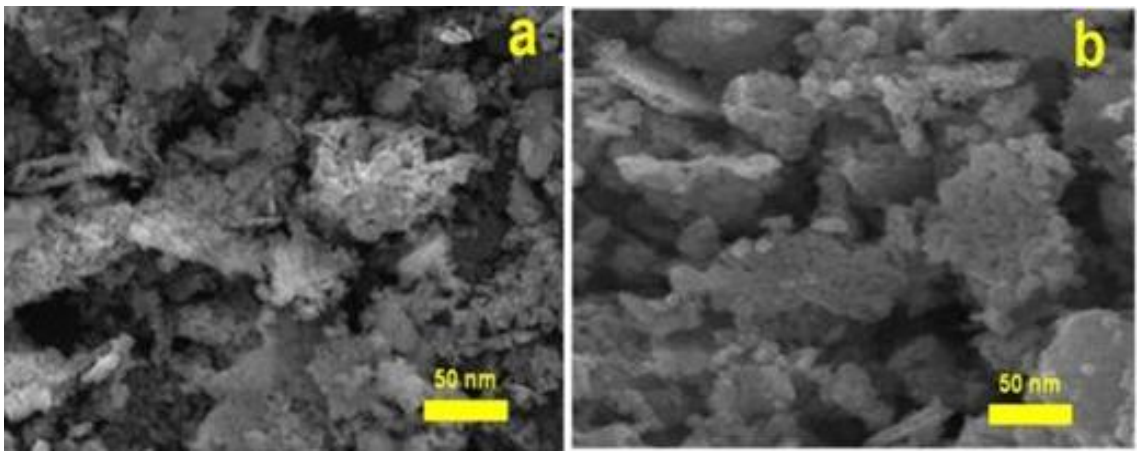

The FE-SEM was linked to an EDS/INCA 350 (energy dispersive X-ray analyzer) manufactured by Oxford Instruments Ltd. The structural changes were observed by ABB Bomem MB 102 infrared spectrometer. The samples were mixed with KBr and made in the form of pellets and recorded at 4 cm^{-1} resolution. Magnetic measurements were performed using Lakeshore VSM 7410 at room temperature with maximal applied magnetic fields of 10 kOe. Maximum magnetization, coercivity and remanent magnetization were observed from the hysteresis loops.

3. RESULTS AND DISCUSSION

3. 1. Magnetic properties

Hysteresis loops for zinc substituting $CuFe_2O_4$ nanoferrites at room temperature are shown in Figure 2. The values of saturation magnetization (M_s), coercivity (H_c) and remanence (M_r) are given in Table 1.

The magnetic properties of Cu-Zn nanoferrites vary with changing zinc content. The variation of magnetic properties of $Cu_{1-x}Zn_xFe_2O_4$ nanoferrites can be understood in term of cation distribution and exchange interactions between spinel lattices. The $Cu_{1-x}Zn_xFe_2O_4$ nanoferrites with $x \leq 0.6$ exhibit ferromagnetic behavior, whereas for $x = 1.0$ nanoferrites display paramagnetic character with zero coercivity, zero remanence and non-saturated magnetization.

Figure 2. Hysteresis curves for the samples $Cu_{1-x}Zn_xFe_2O_4$ ($0.2 \leq x \leq 1.0$) nanoparticles.

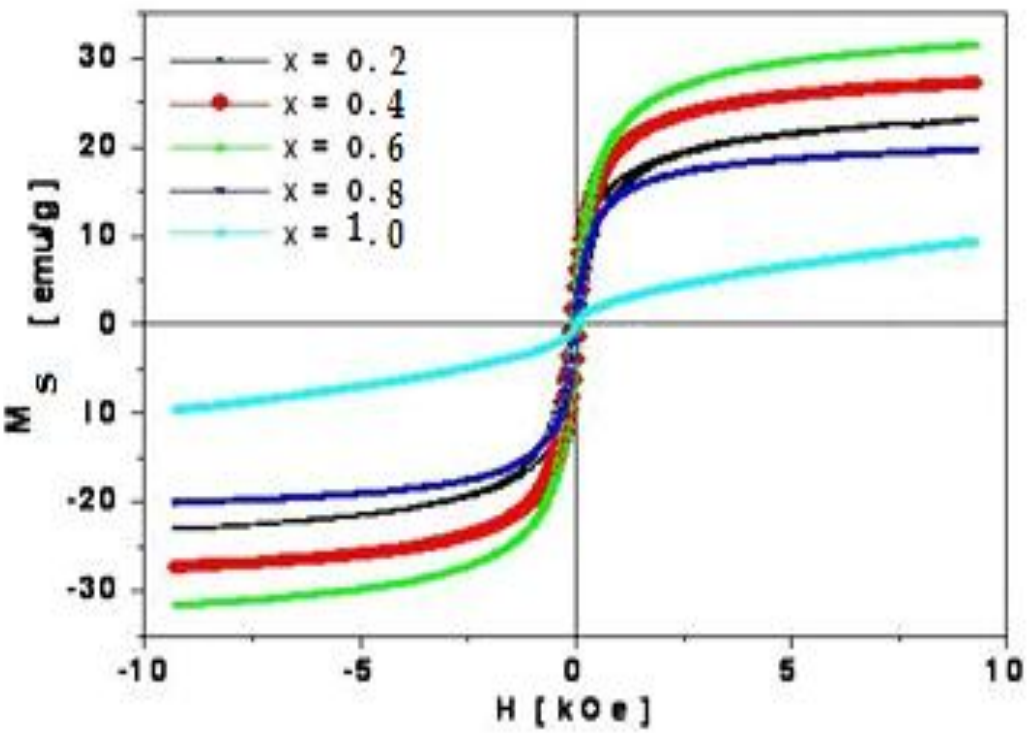

Table 1. Coercivity H_c, remanence magnetization M_r, maximum magnetization at M, for $Cu_{1-x}Zn_xFe_2O_4$ ($0.2 \leq x \leq 1.0$) nanoparticles.

x	H_c [Oe]	M_r [emu/g]	M_s [emu/g]
0.2	133	5.9	26.7
0.4	147	7.6	33.5
0.6	95	6.5	39.5
0.8	76	3.5	28.3
1.0	25	1.2	10.6

The saturation magnetization initially increases with increasing zinc content and reaches a maximum (39.5 emu/g) and then decreases. The increase in saturation magnetization may be attributed to the fact that, small amount of Zn ions substituted for Cu occupy A sites displaces Fe ions from A sites to B sites, which increases the content of Fe ions in B sites. This leads to an increase of magnetic moment in B-site and a decrease of magnetic moment in A-site. So the net magnetization increases, which is consistent with the increase of saturation magnetization. With further increase nonmagnetic Zn ions substitution, the dilution at the A sites increases.

This results in the breakdown of the ferromagnetic phase at $x \leq 0.6$. For $Cu_{1-x}Zn_xFe_2O_4$ ($x = 0.8$ and 1.0), the triangular spin arrangement on B-sites is suitable and this causes a reduction in A-B interaction and an increase of B-B interaction. Therefore, the decrease of saturation magnetization can be explained on the basis of three sublattice model (Yafet and Kittle, 1952). As shown in Table 1, coercivity (H_c) continuously reduced with increasing Zn ions content. These magnetic behaviors of ferrite depend entirely on the spinel structure. For instance, normal spinel ferrite shows an antiferromagnetically ordering, while inverse spinel ferrite shows a ferromagnetic ordering. With increasing Zn ions concentration, a transformation from inverse spinel structure of $CuFe_2O_4$ ferrite to normal spinel structure of $ZnFe_2O_4$ ferrite wills arises gradually. Variation of saturation magnetization with Zn content is as shown in Figure 3.

The observed variations can be explained on the basis of cations distribution and exchange interaction between Fe ions and between Zn ions at the tetrahedral A and octahedral B sites. When Zn ions are introduced at the expense of Cu ions, some of the Fe ions migrate from A – to the B- sites. This increases the Fe ion concentration at B-sites. As a result, the magnetic moment of B sub-lattices increases with increasing Zn concentration up to $x \leq 0.6$. However, as Zn concentration increases, the Fe ions left at A-site being small in number, the A–B interaction experienced by B-site iron ions decreases. Also, the increased number of Fe ions at the B-site increases the B–B interaction, resulting in spin canting (Kakatkar *et al.*, 1996). The decrease in the B sub-lattice moment, interpreted as a spin departure from co-linearity, causes the effect known as canting. Magnetization values for the present Cu-Zn nanoferrites were observed to be smaller than that of ceramically prepared samples (Sattar *et al.*, 2005). This might be due to several reasons such as Nanocrystalline nature, surface disorder, modified cationic distribution etc. (Parvatheeswara Rao *et al.*, 2007).

Figure 3. Maximum magnetization values observed for $Cu_{1-x}Zn_xFe_2O_4$ ($0.2 \leq x \leq 1.0$) nanoparticles from hysteresis loops.

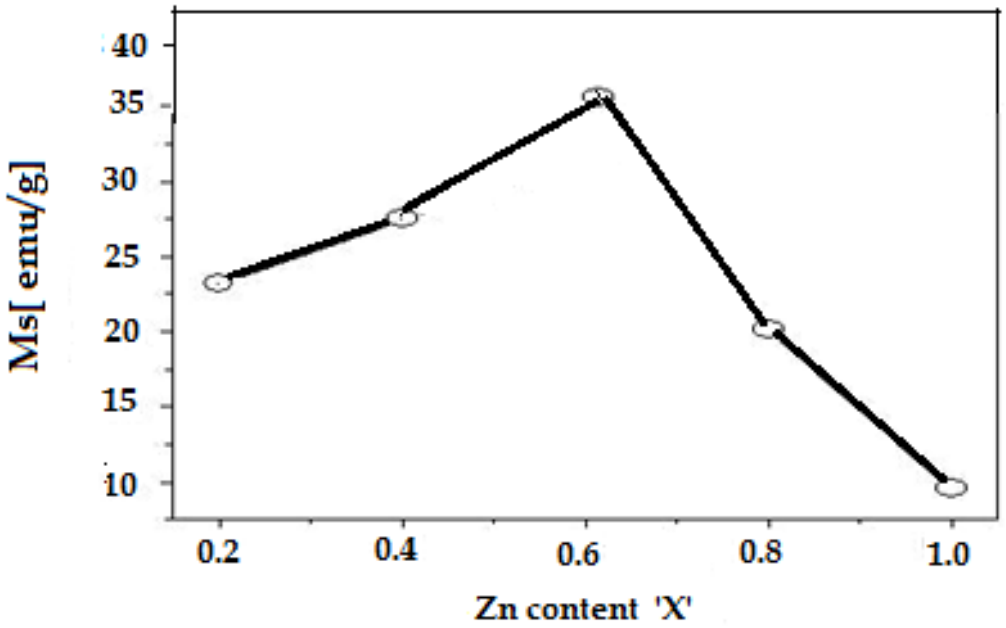

Figure 4 shows the change in the coercive force (H_c) with Zn ion concentration. The coercivity is influenced by factors such as magneto crystalline anisotropy, micro-strain, magnetic particle morphology, size distribution, shape anisotropy, and magnetic domain size. The magnitude of H_c decreases with increase in Zn content. This behavior is similar to that of porosity. Porosity affects magnetization process because pores work as a generator of demagnetizing field.

Figure 4. Coercivity (H_c) values observed for $Cu_{1-x}Zn_xFe_2O_4$ ($0.0 \leq x \leq 0.8$) nanoparticles.

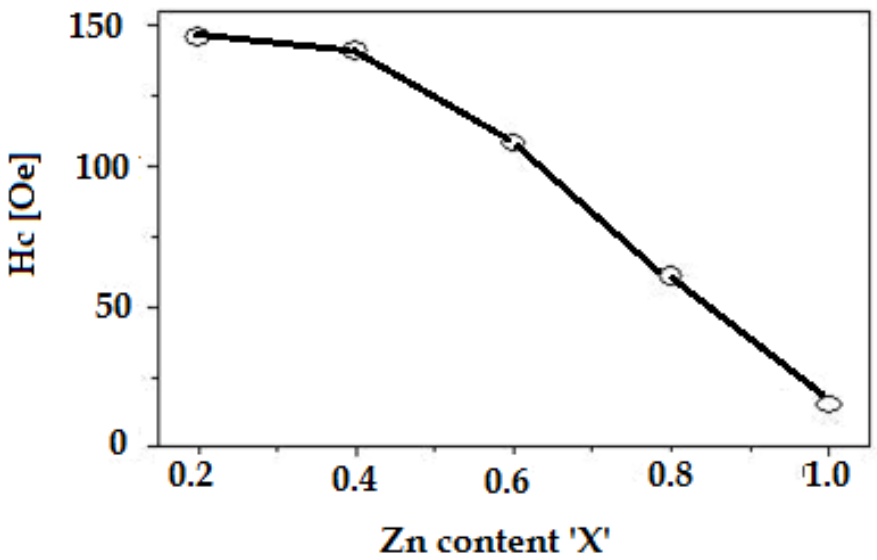

As the porosity decreases high field is needed to push the domain wall and thus Hc decreases. It is known that the coercive force has a direct relation with the anisotropy constant of the sample, and, according to the one ion model, the anisotropy field of ferrites depends on the amount of Fe ions in the sample (Chikazumi and charap, 1964; Coey, 1996). In the present study, it seems that the amount of Cu^{2+} ions decreases as a result of increase in Zn^{2+} content. This means that the magneto anisotropy constant decreases with increase in Zn content and that, consequently, the magnitude of H_c also decreases. The observed magnetic properties of Cu-Zn nanoferrites were due to the combined effect of reduced particle size as well as with the increase of non-magnetic Zn content.

4. CONCLUSION

A series of $Cu_{1-x}Zn_xFe_2O_4$ ($0.2 \leq x \leq 1.0$) nanoparticles were prepared using precursor method. The XRD analysis reveals the formation of single phase spinel structure at very low annealing temperature without any secondary phases. The particle size was observed to decrease with increasing Zn concentration probably due to the reaction temperature and time. The lattice parameters were observed to increase with increasing Zn content *x*, which is due to large ionic radii of zinc when compared to copper ions. Magnetic measurements at room temperature for these samples revealed that magnetization at $\approx 1T$ do not change monotonically with the change of Zn content *x*. The coercivity and remanence decreases with increasing non-magnetic Zn content *x*.

References

[1] Ashok R.L., Jayanna H. S., Parameshwara P., Somasekhar R., *Indian Journal of Pure and Applied Physics* 47(10) (2009) 715-719.

[2] Auzans E., Zins D., Blums E., Massart R., *Journal Material Science* 34 (1999) 1253-1260.

[3] Chikazumi S and Charap S (1964). *Physics of Magnetism.* John Wiley and Sons, New York, p. 140.

[4] Coey J. M. D. (1996). *Rare Earth Permanent Magnetism* John Wiley and Sons, 1st edition New York, p. 220.

[5] Faungnawakij K., Tanaka Y., Shimoda N., Fukunaga T., Kikuchi R., Eguchi K., *Applied Catalysis* B74 (2007) 144-151.

[6] Kakatkar S. V., Kakatkar S. S., Patil R. S., Sankpal A. M., Suryawanshi S. S., Bhosale D. N., Sawant S. R., *Physica Status Solidi* B198 (1996) 853-860.

[7] Parvatheeswara Rao B., Caltun O., Cho W. S., Chong-Oh Kim, Cheol Gi Kim, *Journal of Magnetism and Magnetic Materials* 310 (2007) e812-e814.

[8] Patange S. M., Shirsath Sagar E., Toksha B. G., Jadhav S. S., Shukla S. J., Jadhav K. M., *Applied Physica* A95(2) (2009) 429-434.

[9] Pradhan S. K., Bid S., Gateshki M., Petkov V., *Materials Chemistry and Physics* 93 (2005) 224-230.

[10] Raghavender A. T., Pajic D., Zadro K., Milekovic T., Venkateshwar Rao P., Jadhav K. M., Ravinder D., *Journal of Magnetism and Magnetic Materials* 316 (2007) 1-7.

[11] Raghavender A. T., Shirsath S. E., Vijaya Kumar K., *Journal of Alloys and Compounds* 509(25) (2011)7004-7008.

[12] Sattar A. A., El-Sayed H. M., El-Shokrofy K. M., and El-Tabey M. M., *Journal of Materials Engineering and Performance* 14(1) (2005) 99-103.

[13] Smit J., Wijn H. P. J., *Ferrites* _Philips Technical Library, Eindhoven, 1959.

[14] Sugimoto M., *Journal of the American Ceramic Society* 82 (1999) 269-280.

[15] Suzuki Y., *Annual Review of Material Research* 31 (2001) 265-289.

[16] Tanaka T., *IEEE Transactions on Magnetics* 35 (1999) 3010-3012.

[17] Tao S. W., Gao F., Liu X. Q., and Sørensen O.T., *Materials Science and Engineering* B77(2) (2000) 172-176.

[18] Tsoncheva T., Manova E., Velinov N., Paneva D., Popova M., Kunev B., *Catalysis Communications* 12(2) (2010) 105-109.

[19] Wickham D. G., *Inorganic Synthesis* 9 (1967) 152.

[20] Yafet Y., Kittel C., *Physical Review* 87 (1952) 290-294.

[21] Yao C. W., Zeng Q. S., Goya G. F., Torres T., Liu J. F., Jiang J. Z., *Journal of Physical Chemistry* C111 (2007) 12274-12278.

[22] Zuo X., Yang A., Vittoria C., Harris V. G., *Journal of Applied Physics* 99 08M909 (2009).

(Received 14 September 2013; accepted 18 September 2013)